

Physico-chemical and thermochemical studies of the hydrolytic conversion of amorphous tricalcium phosphate into apatite

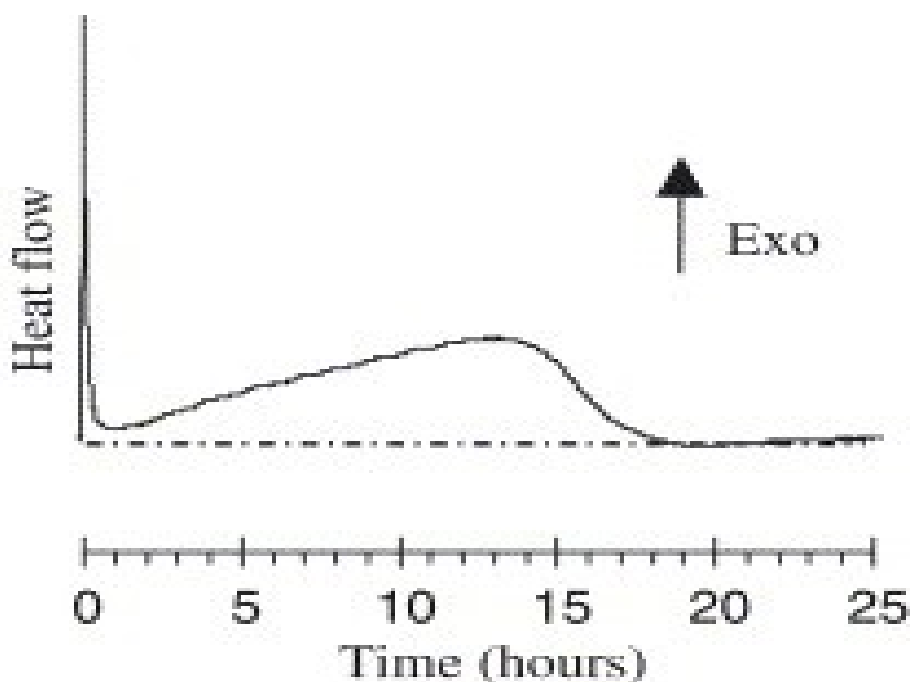
Saida Somrani, Mihai Banu, Mohamed Jemaland Christian Rey

IPEIT, 2 rue Jawar El Nehri, Monfleury, 1089 Tunis, Tunisie
CIRIMAT, Ecole Nationale Supérieure des Ingénieurs en Arts Chimiques et Technologiques,
INPT-ENSIACET, UMR CNRS 5085, 118 route de Narbonne, 31077 Toulouse cedex 4, France
Laboratoire de Thermodynamique Appliquée, Département de Chimie, Faculté des Sciences,
Campus Universitaire, Tunis 1060, Tunisie

Abstract

The conversion of amorphous tricalcium phosphate with different hydration ratio into apatite in water at 25 °C has been studied by microcalorimetry and several physical–chemical methods. The hydrolytic transformation was dominated by two strong exothermic events. A fast, relatively weak, wetting process and a very slow but strong heat release assigned to a slow internal rehydration and the crystallization of the amorphous phase into an apatite. The exothermic phenomenon related to the rehydration exceeded the crystalline transformation enthalpy. Rehydration occurred before the conversion of the amorphous phase into apatite and determined the advancement of the hydrolytic reaction. The apatitic phases formed evolved slightly with time after their formation. The crystallinity increased whereas the amount of HPO_4^{2-} ion decreased. These data allow a better understanding of the behavior of biomaterials involving amorphous phases such as hydroxyapatite plasma-sprayed coatings.

Graphical abstract



The hydrolytic evolution of amorphous tricalcium phosphate shows two main exothermic events corresponding to wetting of the particle surface and to a slow inner rehydration associated with crystallization. These data allowed the determination of the rehydration and crystalline transformation enthalpies.

Keywords: Amorphous calcium phosphate; Apatite; Hydrolysis; Crystallization; Microcalorimetry; Enthalpies

1. Introduction
 2. Materials and methods
 - 2.1. Synthesis and thermal treatment of lyophilized amorphous tricalcium phosphate
 - 2.2. Hydrolytic treatment of ATCPs and experimental techniques
 3. Results
 - 3.1. Characteristics of starting samples
 - 3.2. Microcalorimetric curves
 - 3.3. Characteristics of the hydrolytic-treated samples
 - 3.3.1. Chemical composition
 - 3.3.2. X-ray diffraction
 - 3.3.3. Infrared spectroscopy
 - 3.3.4. DTA results
 - 3.3.5. TGA results
 - 3.3.6. Solution evolution
 4. Discussion
 - 4.1. Physical and chemical transformations during the hydrolytic treatment
 - 4.2. Enthalpy variations during the hydrolytic treatment
 - 4.2.1. The first peak
 - 4.2.2. The second peak and the endothermic peak
 5. Conclusion
- Acknowledgements
References

1. Introduction

Although they do not seem to exist in detectable amounts in hard tissues of vertebrates amorphous calcium phosphates (ACPs) have been observed in many biological systems [1], [2] and [3]. They also appear as a transient or constitutive phase in many commercial calcium phosphate biomaterials such as plasma sprayed coatings of metal orthopedic prostheses and orthopedic cements [4], [5], [6], [7], [8] and [9] and they have been shown to form at the very beginning of surface reactions occurring in implanted bioglasses [10]. In plasma sprayed coatings, ACPs have been found to play a major role in the mechanical properties of the coatings, especially their adhesion to metal surfaces [11] and [12] and their biological properties [13], [14] and [15]. Thus, an increase of the ACP content of a coating improves its osteoconductive properties (i.e. the propensity of the material to favor bone growth when it is in contact with bone tissue); however, this labile, metastable and rather soluble phase also promotes, concomitantly, the degradation of the material impairing its biological integration into the tissue [8], [13], [14], [15] and [16]. This drawback has led to various attempts to limit and control the amount of ACPs in coatings, using their ability to become converted into apatites either by dry heating [17] and

[18], or by treatment in aqueous media [5]. The apatitic conversion of ACPs is also involved in the setting reactions of Ca–P cements and invariably occurs when ACP-containing materials are implanted in the living body [9], [19] and [20]. Although the conversion of ACPs into apatites has been studied by several authors in different conditions [21], [22], [23], [24], [25], [26] and [27], very few studies have aimed to determine the thermochemical events associated with these rather complex reactions [28], [29], [30] and [31]. Moreover, these studies were performed on wet ACPs which are different from the dry, pre-heated, ACPs found in commercial hydroxyapatite (HA) coatings and Ca–P cements.

A recent work [32] has shown that pre-heated ACP samples exhibit very different dissolution enthalpies suggesting that the hydrolysis of ACP phases could follow different pathways depending on their preparation conditions. The purpose of this study was to analyze the physico-chemical and the thermochemical events occurring during the hydrolytic treatment of different amorphous tricalcium phosphates (ATCPs) obtained by lyophilization and pre-heated at different temperatures.

2. Materials and methods

ACPs vary widely in composition. Many different ACPs with atomic Ca/P ratios ranging from 1.15 to 1.67 and higher have been described [33], [34], [35], [36], [37] and [38]. ATCP (Ca/P=1.50), however, seems particularly stable [26] and is easily formed by double decomposition [21], [30] and [39]. This phase is one of the best known ACPs and has been chosen for our study.

2.1. Synthesis and thermal treatment of lyophilized amorphous tricalcium phosphate

ATCP was obtained by double decomposition of freshly mixed aqueous solutions of soluble calcium and phosphate salts [39]. A calcium nitrate solution (46.3 g $\text{Ca}(\text{NO}_3)_2 \cdot 4\text{H}_2\text{O}$ dissolved in 0.550 L of deionized water containing 40 mL of 28% weight ammonia solution) was rapidly poured into an ammonium phosphate solution (27.2 g $(\text{NH}_4)_2\text{HPO}_4$ dissolved 1.300 L of deionized water containing 40 mL of 28% weight ammonia solution). The precipitate formed was immediately filtered on büchner funnels and washed with 3.0 L of deionized water containing 15 mL of 28% weight ammonia solution. After washing, the gel sample was lyophilized during 72 h (Heto[®] CT60c). All lyophilized ATCP (ATCP_{ly}) samples were stored at –18 °C between experiments to avoid any spontaneous transformation.

ATCP samples pre-heated to 200 and 400 °C were selected based on the results of a previous study on the dissolution enthalpies of these phases [32]. The heating temperature is indicated as a subscript: ATCP₂₀₀ and ATCP₄₀₀. The lyophilized samples were placed in an alumina crucible and introduced into a pre-heated oven at different temperatures for two hours. They were then cooled in air at room temperature in desiccators and stored in a freezer at –18 °C.

2.2. Hydrolytic treatment of ATCPs and experimental techniques

The conversion of ATCP into apatite was obtained after immersion in deionized water with a liquid-to-solid weight ratio of 100. The standard enthalpy variations were measured using an isothermal microcalorimeter (C-80 seteram[®]) at 25 °C. The reaction vessel was composed of two separate compartments containing the powder and the liquid, respectively. The precise mass, about 40.00 (±0.02) mg, of powder sample was introduced in the lower measuring compartment. The upper compartment was filled with 0.50 (±0.01) mL of mercury and 4.00 (±0.05) mL of

distilled water. The mercury was added to prevent any contact between the water vapor and the powder during equilibration of the calorimeter. The reference cell contained 0.50 (± 0.01) mL of mercury and 4.00 (± 0.05) mL of distilled water. The thermal flow equilibrium was obtained after 12 h. Then, the whole microcalorimeter was tipped over for a few minutes in order to disperse the powder in the water. The thermal flow was recorded for at least 24 h. The different peaks were integrated to calculate the heat exchanged. Peak separation was done using the “ballistic method” [40], which allows the separation of narrow and broad peaks and seems particularly suited to the determination of the heat effect associated with the first phenomenon.

To analyze the phase transformation more accurately, the hydrolytic treatments were interrupted at various time intervals. Indeed for each of the ATCP studied, about 20 separate essays were carried out at chosen times. In every essay 200 mg of powder were immersed into 20.0 mL of deionized water. The hydrolysis was carried out at 25.0 (± 0.5)°C in hermetically closed flasks to prevent water evaporation and to minimize carbonate uptake from atmospheric CO₂. These experiments lasted from 30 min to three days. The precipitate was separated from the solution by filtering; and was washed with deionized water and lyophilized.

The infrared spectra of the lyophilized samples were recorded on a Perkin-Elmer 1760[®] FTIR spectrometer from samples embedded in KBr pellets. The data were analyzed using Grams 32 software[®].

X-ray diffraction patterns (XRD) were obtained on a curved counter (CPS 120 INEL[®]) using the K_α radiation of a Co anticathode. The apparent dimensions of the crystals formed just after the hydrolytic transformation were calculated using Scherrer's formulae [41].

The rate of conversion was determined using the crystallization peak of ATCP [42]. A precise mass—18.00 (± 0.05) mg—of each sample obtained before and during the hydrolytic treatment was placed in a platinum crucible. It was submitted to differential thermal analysis (DTA) under a U-grade argon flow with a linear temperature increase of 15 K/min with a SetSys16/19-seteram[®] apparatus. In these experimental conditions, the crystallization peak of the ATCP was observed around 626 °C. The peak area, proportional to the crystallization enthalpy of the ATCP phase, was integrated by seteram[®] software. If $A_{t_0}\langle\text{ATCP}\rangle$ represents the area of the crystallization peak of the initial amorphous phosphate and $A_t\langle\text{ATCP}\rangle$ the area of the crystallization peak of the residual lyophilized amorphous phase contained in calcium phosphate after hydrolytic treatment for different times ‘ t ’, the crystalline fraction is:

$$\langle\xi_{\text{cryst}}\rangle = [A_{t_0}\langle\text{ATCP}\rangle - A_t\langle\text{ATCP}\rangle] / A_{t_0}\langle\text{ATCP}\rangle.$$

The estimated value of the standard deviation of this method is ± 0.06 .

For each of these samples, the water content was determined by thermal gravimetric analysis (TGA) on a TG92-seteram[®] instrument in the same conditions as for DTA. It corresponds to TG-loss recorded between 50 and 500 °C [32] and [39].

The chemical analyses were performed on each lyophilized and pre-heated ATCP sample at different stages of hydrolytic treatment in order to determine a possible evolution of the Ca/P ratio, as reported by several authors. The calcium was determined by complexometry with ETDA [43] and the total-phosphorus content and the HPO₄²⁻ amount were analyzed according to the protocol proposed by Gee and Dietz [44]. The samples were heated at 600 °C during 20 min to convert the HPO₄²⁻ ions into pyrophosphate P₂O₇⁴⁻ and then a spectrophotometry of the phosphovanadomolybdic acid was performed before and after hydrolysis of the pyrophosphate moiety. Traces of magnesium, present in the initial synthesized ATCP were analyzed by

absorption spectrometry in the presence of lanthanum chloride [43]. The very low amounts of carbonate in the samples were determined by coulometry [45] using a UIC-Coulometrics[®] apparatus.

Some hydrolysis solutions were also analyzed mainly at the beginning of hydrolytic treatment, and after 15, 30, and 60 min of immersion. These experimental times were chosen to obtain information about the dissolution behavior of ATCP and the supersaturation of the solution with respect to different Ca–P compounds. The phosphorus content was determined as for solid samples by spectrophotometry of phosphovanadomolybdic acid [44] and the calcium content by Atomic Absorption spectrometry in the presence of lanthanum chloride [43].

3. Results

3.1. Characteristics of starting samples

The results of chemical analysis of the starting ATCP samples are reported in [Table 1](#). The atomic Ca/P ratio corresponds to that of tricalcium phosphate. As usually found in these syntheses, a very small amount of magnesium (originally contained in the reagent grade calcium nitrate used for the synthesis) and carbonate ions (from the air) were evidenced.

Table 1.

Chemical composition of the initial lyophilized ATCP

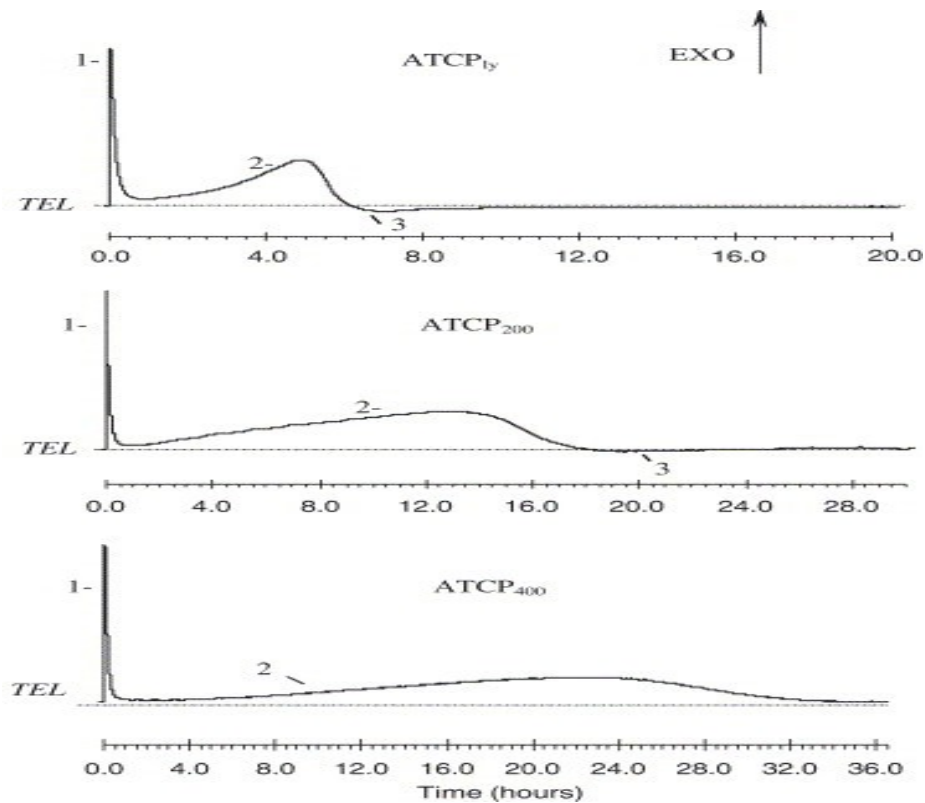
Ca (% in weight)	P (% in weight)	Mg (% in weight)	CO ₃ (% in weight)	Atomic C/P	Atomic Mg/Ca	Atomic Ca/P	Atomic (Mg+Ca)/(C+P)
32.37±0.15	16.66±0.04	0.68±0.08	0.52±0.04	0.016±0.001	0.035±0.006	1.50±0.01	1.53±0.02

During the heating of the starting ATCPs, the water losses were recorded. The TGA-data indicate that ATCP_{1y}, ATCP₂₀₀ and ATCP₄₀₀ contained, respectively 16.5, 6.3 and 3.7 wt% of water. The pre-heated samples were analyzed by FTIR and XRD. They kept the characteristic features of amorphous Ca–P as reported earlier [32].

3.2. Microcalorimetric curves

[Fig. 1](#) represents the microcalorimetric curves of the lyophilized sample and those pre-heated at 200 and 400 °C. These curves exhibit the same characteristic features. Each curve seems to be essentially composed of two main exothermic peaks.

Fig. 1. Isothermal microcalorimetric curves at 25 °C for the hydrolytic treatments of the lyophilized and pre-heated ATCPs in deionized water: (1) first peak, (2) second peak, (3) endothermic peak and, TEL: Representation of the Thermal Equilibrium Line.



The first asymmetrical rather sharp exothermic peak begins as the powder enters in contact with water. Its maximum is reached in about 2 min and its intensity slowly decreases and reaches a minimum after about 50 min.

The second peak appears much wider and more asymmetrical. It is associated with a much slower process than the first one. The length of this event depends strongly on the heat treatment received by the studied ATCP: the phenomenon lasts about 6 h 30 min for the lyophilized sample, 17 h 30 min for the sample pre-heated at 200 °C and up to 30 h for the sample pre-heated at 400 °C.

The standard enthalpies measured exhibited strong variations owing to the pre-heating treatment of the ATCP samples (Table 2). The enthalpy of the first peak was much weaker than that of the second. Besides, its amplitude varied only slightly for all samples although its length seemed to increase a little with the ATCP heating temperature. In contrast, the enthalpy from the second peaks varied considerably and appeared more exothermal for the pre-heated samples than for the lyophilized ones.

Table 2.

Standard enthalpy variations during the hydrolytic treatment at 25 °C in deionized water of the lyophilized and pre-heated ATCPs

Studied sample	Total enthalpy-Apatitic conversion enthalpy (J g^{-1} ($\pm 1\%$))	First peak-Wetting phenomenon-		Second peak (J g^{-1} ($\pm 2\%$))
		Length (min)	Enthalpy (J g^{-1} ($\pm 1\%$))	
Lyophilized	-85.3	39	-11.3	-74.0
Pre-heated at	-193.0	54	-11.6	-181.4

Studied sample	Total enthalpy-Apatitic conversion enthalpy (J g ⁻¹ (±1%))	First peak-Wetting phenomenon-		Second peak (J g ⁻¹ (±2%))
		Length (min)	Enthalpy (J g ⁻¹ (±1%))	
200 °C				
Pre-heated at 400 °C	-205.2	56	-11.6	-193.6

After the exothermic peaks, an endothermic peak was sometimes detected fading slowly away (Fig. 1). This phenomenon might have started before it was detected and could have been overlapped by the preceding exothermic peak.

3.3. Characteristics of the hydrolytic-treated samples

3.3.1. Chemical composition

The chemical composition of the hydrolyzed samples is reported in Table 3. The atomic Ca/P ratios appear slightly lower than those of the starting samples, the most obvious change during the hydrolytic treatment was the formation of HPO₄²⁻ entities, as already observed by several authors [24], [26], [30], [46], [47], [48] and [49]. The Ca/P ratio increased very slightly during the hydrolytic treatment or remained constant.

Table 3.

Chemical composition of the lyophilized apatitic products obtained after immersion of the initial amorphous samples in deionized water at 25 °C during different periods

Initial amorphous sample—Chemical formulae	Immersion time/h	Lyophilized apatitic product obtained after immersion	
		HPO ₄ ²⁻ content molar % total P (±0.8)	Ca/P _t (atomic ratio for total P) (±0.01)
Lyophilized-Ca ₃ (PO ₄) ₂ , 3.5 H ₂ O-	12.5 ^a	9.3	1.4
	72	7.7	1.3
Pre-heated at 200 °C-Ca ₃ (PO ₄) ₂ , 1.2 H ₂ O-	22 ^a	10.1	1.4
	72	7.8	1.3
Pre-heated at 400 °C-Ca ₃ (PO ₄) ₂ , 0.6 H ₂ O-	32 ^a	10.1	1.4
	72	8.8	1.4

Initial amorphous sample— Chemical formulae	Immersion time/h	Lyophilized apatitic product obtained after immersion	
		HPO ₄ ²⁻ content molar % total P (±0.8)	Ca/P _t (atomic ratio for total P) (±0.01)
Ca ₃ (PO ₄) ₂ , 1.2 H ₂ O	72	7.8	1.52
Pre-heated at 400 °C- Ca ₃ (PO ₄) ₂ , 0.6 H ₂ O	32 ^a	10.1	1.49
	72	8.8	1.49

^a Corresponds to the end of the hydrolytic conversion.

3.3.2. X-ray diffraction

The XRD data give very similar results for all the samples. As an example, the evolution of the patterns of ATCP₂₀₀ during its hydrolytic treatments is reported in Fig. 2. At the beginning only the very broad halos characteristic of ATCP are observed. As time elapses the ATCP halos decreased in intensity and broad peaks characteristic of poorly crystalline apatites progressively appeared. No transient formation of other crystalline phases such as octacalcium phosphate (OCP), frequently reported as a hydrolysis intermediate of ATCP [23], [24], [26] and [50], was detected. At the end of the conversion period only the broad peaks of a poorly crystalline apatite phase were observed. The most important difference between the ATCP samples was in the duration of the conversion which increased in pre-heated samples.

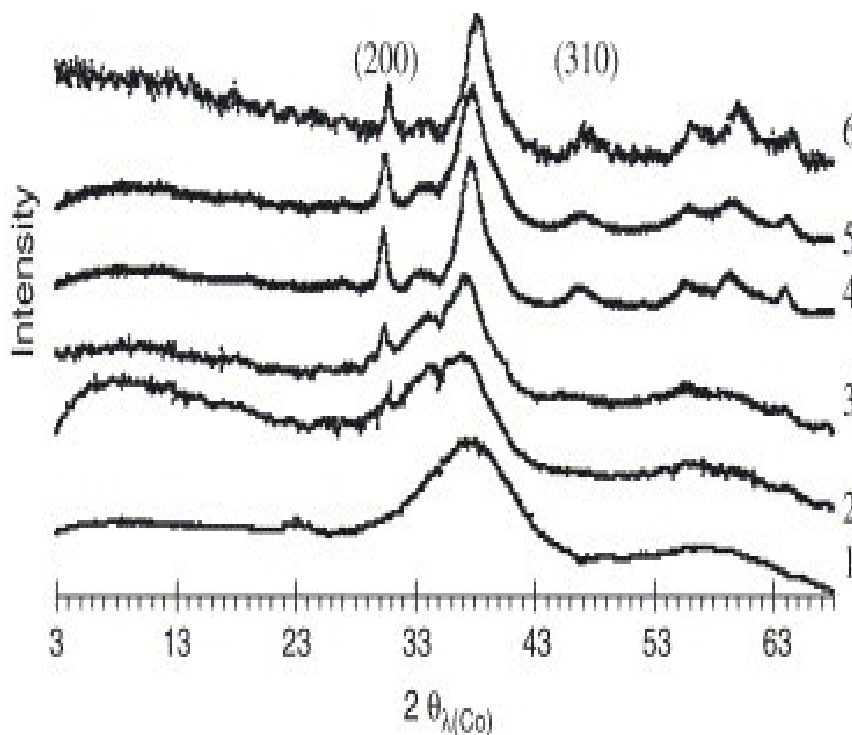


Fig. 2. Evolution of XRD diagrams during the isothermal hydrolytic treatment at 25 °C of the ATCP pre-heated at 200 °C: (1) 0, (2) 4, (3) 10, (4) 14, (5) 20 and, (6)

48 h.

The average and apparent size of the apatitic crystals was determined from XRD peak broadening just after the hydrolytic conversion (Table 4). Although other parameters are involved in this broadening, this simple method gives a good description of the formed crystals. All samples showed an elongation along the *c*-axis of the hexagonal structure as usually found for bone mineral crystals and poorly crystalline apatites [51]. There were no differences between the apatites formed from the different ATCP samples.

Table 4.

Average apparent size of the apatitic crystallites formed just after the hydrolytic apatitic conversion at 25 °C in deionized water of the lyophilized and pre-heated

Apparently size	Studied sample		
	Lyophilized	Pre-heated at 200 °C	Pre-heated at 400 °C
ATCPs $L_{(002)} (\pm 5) (\text{Å})$	129	133	135
$L_{(310)} (\pm 5) (\text{Å})$	40	36	44

Apparently size	Studied sample		
	Lyophilized	Pre-heated at 200 °C	Pre-heated at 400 °C
$L_{(002)} (\pm 5) (\text{Å})$	129	133	135
$L_{(310)} (\pm 5) (\text{Å})$	40	36	44

3.3.3. Infrared spectroscopy

The spectra of the apatitic samples after total conversion indicate the close analogy of the hydrolyzed products (Fig. 3). The spectra are characteristic of poorly crystalline, weakly carbonated apatites [51] and [52]. The bands assigned to OH^- and HPO_4^{2-} groups are distinctly observed. In order to get a more precise evaluation of the characteristics of the apatitic phase, the $\nu_4 \text{PO}_4^{3-}$ band was decomposed into elementary bands corresponding, respectively, to OH^- (633 cm^{-1}), labile phosphate (617 cm^{-1}), apatitic phosphate ($600, 578$ and 560 cm^{-1}) apatitic HPO_4^{2-} (550 cm^{-1}) and labile HPO_4^{2-} (534 cm^{-1}) [20]. The results indicate that the fastest hydrolyzed ATCP produced the most immature apatite rich in labile species (Fig. 4). In addition the formed apatite continued to evolve shortly after total conversion of ATCP into more crystalline, more mature apatites with increased OH^- content as it is usually observed for poorly crystalline apatites. However, this evolution seems to rapidly reach a plateau. Thus, after 24 h, the hydrolyzed sample does not seem to change any more (Fig. 4). At any conversion time, the specific bands of OCP, frequently proposed as an hydrolysis intermediate, were noticed.

Fig. 3. FTIR spectra of the lyophilized apatites obtained after the hydrolytic conversion at 48 hours of the lyophilized and pre-heated ATCPs in deionized water at 25 °C.

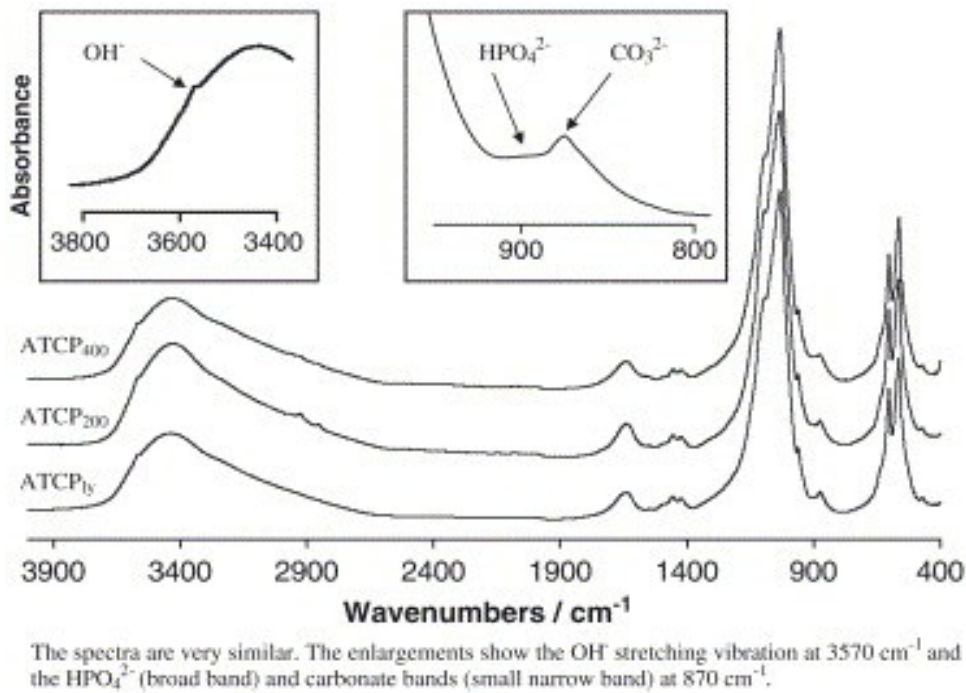
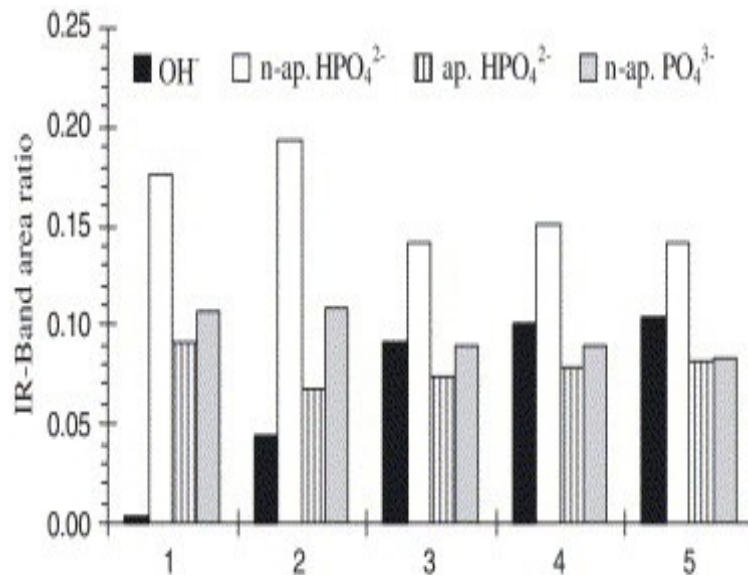


Fig. 4. Band area ratio of OH⁻ ions, non-apatitic (nap.: labile) and apatitic (ap.) HPO₄²⁻ and non-apatitic PO₄³⁻ groups of the lyophilized ATCP after apatitic conversion with hydrolytic treatment times (1) 12 h 30 min, (2) 18 h, (3) 24 h, (4) 48 h and, (5) 96 h.

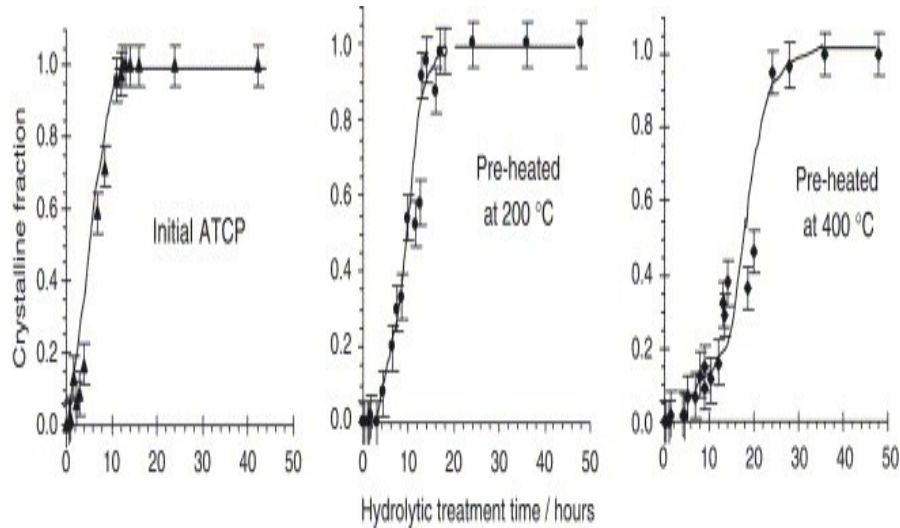


3.3.4. DTA results

The rate of conversion of the different samples, as determined by DTA, is reported in Fig. 5. These curves can be divided into three periods: an “induction period” where the conversion of the ATCP into apatite is barely apparent; a “rapid conversion period”, marked by a rapid decrease of the ATCP fraction; and a gradual “tapering off period”, where the rate of the transformation slows down. Significant ATCP-conversion seems to begin after about 1, 3 and 5 h of immersion for

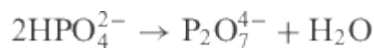
ATCP_{1y}, ATCP₂₀₀ and ATCP₄₀₀, respectively, thus the induction period does seem to depend on the pre-heating treatment of ATCP. The end of the conversion was reached after about 12, 22 and 32 h for ATCP_{1y}, ATCP₂₀₀ and ATCP₄₀₀, respectively.

Fig. 5. Evolution of the crystalline fraction for the lyophilized samples obtained after the hydrolytic treatment at 25 °C in deionized water for different times of the lyophilized and pre-heated ATCPs.



3.3.5. TGA results

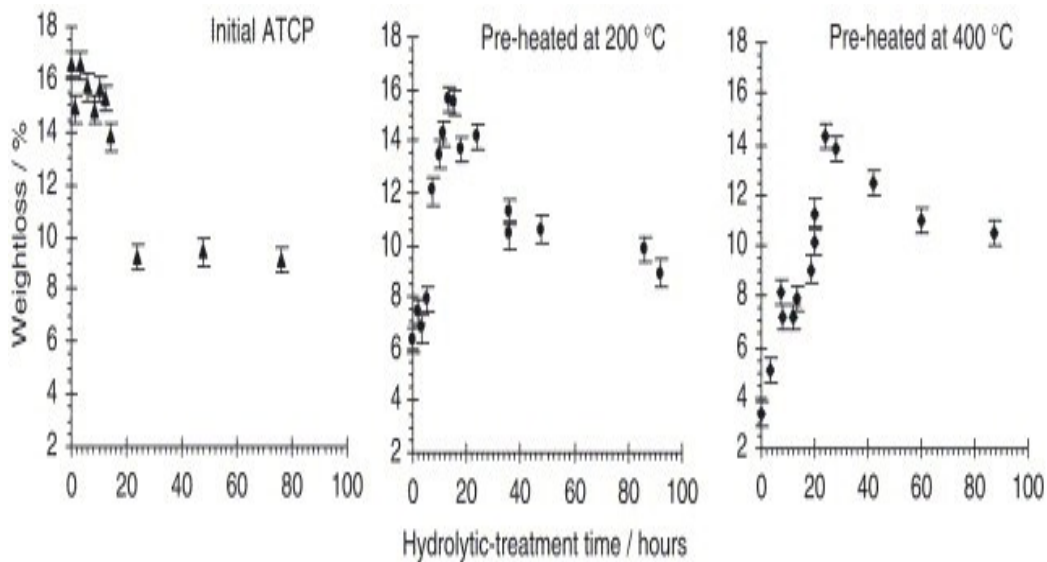
The water loss observed by TGA between 50 and 500 °C corresponds to the water loss through dehydration of the residual untransformed ATCP, to water associated with the hydrolyzed apatitic sample, and to water released due to the condensation of HPO_4^{2-} ions [30] and [39]:



The data presented in [Table 3](#) show that the hydrolysis of PO_4^{3-} into HPO_4^{2-} concerns at most 10% of the phosphate groups. This would release on about 0.6% weight of water. The main loss is thus due to hydration water remaining in the samples after lyophilization associated either to the apatitic or the residual amorphous fraction.

The variation of the water content with hydrolysis time is represented in [Fig. 6](#). For the ATCP_{1y} a significant decrease is observed at the end of the conversion. For ATCP₂₀₀ and ATCP₄₀₀ the water content increased slowly as the advancement of conversion, reached a maximum at the end of the conversion time and then decreased significantly.

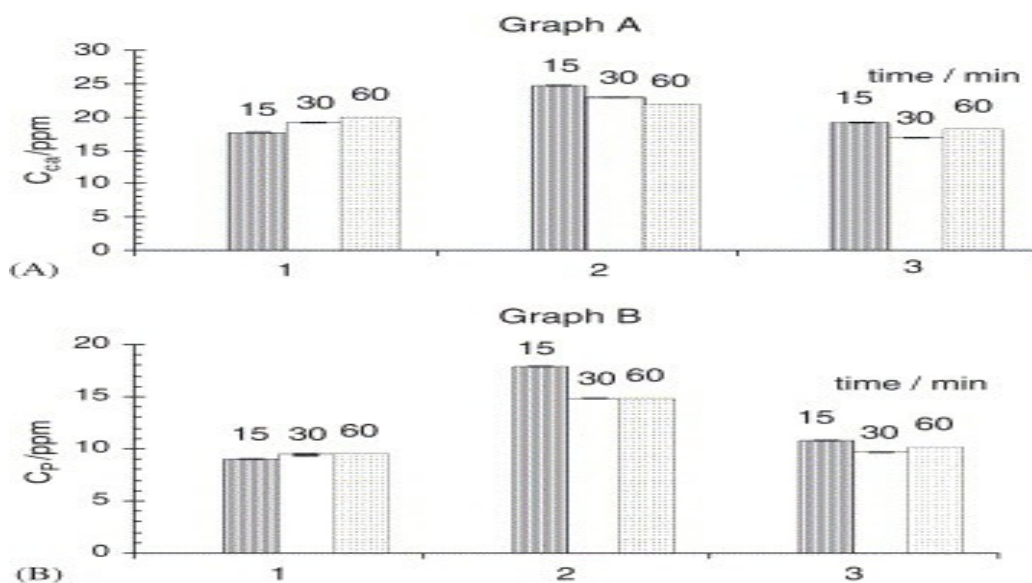
Fig. 6. Evolution of the weight TG-loss, between 50 and 500 °C, of the lyophilized products obtained after the hydrolytic treatments at 25 °C in deionized water for different times of lyophilized and pre-heated ATCPs.



3.3.6. Solution evolution

As shown in Fig. 7, the calcium and phosphate concentrations in the hydrolysis solutions increased rapidly and stabilized at almost constant values, due to the dissolution of the ATCPs. The atomic Ca/P ratios in the solution were significantly different from those of the solid phase. The dissolution is associated with a rise of the pH (up to 10) due to the hydrolysis of dissolved PO_4^{3-} species.

Fig. 7. Variation of the ionic concentrations of calcium (Graph A) and phosphate (Graph B) in hydrolysis solutions obtained after 15, 30 and 60 min of the immersion at 25 °C in deionized water of ATCPs (1) lyophilized, (2) pre-heated at 200 °C and (3) pre-heated at 400 °C.



The ionic-product of the species in solution at the beginning of the hydrolytic treatment was determined for each sample [54] (Table 5). The values obtained indicate that the solution was

oversaturated with respect to OCP and stoichiometric HA but not dicalcium phosphate dihydrate (DCPD) [53]. A solubility-product of each studied ATCP can be calculated from these data, but ATCP phase is not stable enough in solution to reach clear solubility equilibrium.

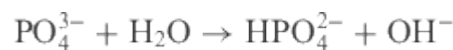
Table 5.

Comparison of the experimental ionic-products of the ATCP hydrolysis solutions (25 °C, 1 h) for some calcium (ortho)phosphate compounds with their solubility products determined at 25 °C

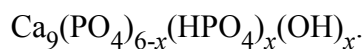
Studied sample	Calcium (ortho)phosphate compound					
	DCPD Ca(HPO ₄)·2H ₂ O		OCP Ca ₄ H(PO ₄) ₃ ·5H ₂ O		HA Ca ₅ (PO ₄) ₃ OH	
	Ionic-product	Solubility product	Ionic-product	Solubility product	Ionic-product	Solubility product
Lyophilized	1.2×10 ⁻⁸		7.5×10 ⁻⁴⁵		3.3×10 ⁻⁴²	
Pre-heated at 200 °C	8.3×10 ⁻⁸	2.1×10 ⁻⁷	2.0×10 ⁻⁴⁴	2.5×10 ⁻⁵⁰	6.8×10 ⁻⁴⁴	4.7×10 ⁻⁵⁹
Pre-heated at 400 °C	2.3×10 ⁻⁸	[59]	9.4×10 ⁻⁴⁵	[59]	6.8×10 ⁻⁴³	[59]

4. Discussion

The conversion of the ATCP gel has been studied by microcalorimetry by Heughebaert and Guegan [29], [30] and [39]. Two distinct phenomena were observed. The first one corresponds to a broad endothermic wave attributed to an internal hydrolysis reaction of the PO₄³⁻ ions of the amorphous phase:



and corresponded to a standard enthalpy 13.5±2.0 kJ mol⁻¹ for Ca₉(PO₄)₆ (i.e. 4.5±0.7 kJ mol⁻¹ for Ca₃(PO₄)₂) at 25 °C. The second one gives a sharp exothermic peak corresponding to the crystallization of ATCP into apatite, its related standard enthalpy was estimated to -3.4±1.0 kJ mol⁻¹ for Ca₉(PO₄)₆ (i.e. -1.1±0.4 kJ mol⁻¹ for Ca₃(PO₄)₂) at 25 °C [29]. It has been observed that, in this system, the ATCP is converted into a non-stoichiometric poorly crystalline apatite with a constant atomic Ca/P ratio of 3/2 [29], [30] and [39]. During the conversion, the HPO₄²⁻ and OH⁻ contents of the solid phase continuously increase and the composition of the latter is given by the following chemical formula:



The variable *x* increases with time. It eventually reaches the theoretical limit, *x*=1, corresponding to an apatitic solid with half filled OH⁻ sites. According to Heughebaert there was a correspondence between the hydrolysis reaction and the crystallization phenomenon.

Other studies performed in different conditions have led to different results. The study of

hydrolytic treatment of ATCP in suspension, and not gels, showed a progressive increase of the atomic Ca/P ratio which was assigned to a dissolution-reprecipitation process, related to the high solubility of the amorphous phase compared to the crystalline apatite [24], [28] and [52]. During this process, the apatite phase could also take up ions present in the solution such as carbonate. This model was suggested to represent what occurs in bone during mineralization of the collagen matrix [55] and [56].

For several authors [46], [47] and [57] the conversion mechanism depends on the pH of the solution. At physiological pH (=7.4) the hydrolysis of ATCP has been described as a two-step process [24]. In the first period a decrease of the atomic Ca/P ratio in the solid phase has been observed (lower than 1.5) associated with an increase of the pH (consumption of acid) and an atomic Ca/P ratio in solution higher than 1.5. The ionic-product in this solution close to the solubility product of OCP has been interpreted as a transient formation of this metastable phase. In the second stage, an increase of the Ca/P ratio of the solid has been observed with consumption of hydroxide ions from the solution and a decrease of the solution's Ca/P ratio. This stage has been interpreted as hydrolysis of the transient OCP phase into apatite by a topotactic reaction leading to an increase in the Ca/P ratio, even though OCP had not been evidenced by the diffraction method. At alkaline pH, however, (above 10.5) the ATCP has been found to convert directly into apatite [57].

The present study brings more information about the chemical processes involved and about the thermal events associated with the hydrolytic-conversion of ATCP phases into apatite.

4.1. Physical and chemical transformations during the hydrolytic treatment

The development of ATCP in aqueous media results in the formation of a poorly crystalline apatite. In the conversion conditions that we used however, there was no evolution of the atomic Ca/P ratio which remained close to 1.50, the initial ratio, like for the transformation into the gel form studied by Heughebaert and Guegan [29], [30] and [39]. The formation of hydrolysis products HPO_4^{2-} and OH^- ions was evidenced by FTIR and chemical analysis.

At any moment, especially at the beginning of conversion, the formation of OCP was undetectable either by FTIR or by XRD. However the analyses of the hydrolysis solutions of the lyophilized ATCP reveals a Ca/P ratio higher than 1.50 at the very beginning of the treatment of the lyophilized sample which might support the transient formation of a solid phase with a Ca/P ratio lower than 1.50. Considering the ionic-product of the solution, this phase could possibly be OCP although the variation observed could also be assigned to an alteration of the composition of the ATCP, involving for example an hydrolysis of the PO_4^{3-} groups and a release of Ca^{2+} . In the case of the samples pre-heated at 200 and 400 °C however the solution analyzes indicate at any stage a Ca/P ratio lower than 1.50 incompatible with transient OCP formation.

Our results seem very close to those Heughebaert and Guegan, but they also differ in several aspects [29], [30] and [39]. In our experimental conditions, we did not reach maximum hydrolysis of PO_4^{3-} ions (15.8₃% of total P). This discrepancy can be related to different experimental conditions and suggests that the rate of hydrolysis is not necessarily related to crystallization. Other discrepancies exist however between our data and those of other authors [24], [28], [47], [52] and [57] who found a variation of the Ca/P ratio of the mineral phase during hydrolysis. These differences could be attributed in part to the variation in the liquid-to-solid ratio, which could considerably affect the composition of the apatitic-phase formed. The increase (or decrease) of the solid Ca/P ratio is necessarily linked to a decrease (or an increase) of that in the solution, to maintain the total composition constant. However, due to the very low solubility of these Ca-P phases, the influence of the amount of ions in the solution on the Ca/P ratio of the solid phase depends strongly on the liquid-to-solid ratio. When this is low, significant changes in the

composition of the solid phase cannot occur due to a very limited amount of ions in the solution which is negligible compared to the amount of ions in the solid phase. On the contrary, in the case of a high liquid-to-solid ratio the amount of ions in the solution cannot be neglected compared to the total amount of ions, therefore strong variations of the solid Ca/P ratio could occur depending on the conditions of phase equilibrium. In order to evaluate this effect hydrolysis were performed at three different liquid/solid ratios (Table 6). The data indicate a small but significant increase of the Ca/P ratio of the solid phase when the liquid/solid ratio becomes very high.

Table 6.

Effect of liquid/solid weight ratio on the composition of formed apatites (13 h at 25 °C, ATCP lyophilized)

Liquid/solid weight ratio	HPO ₄ ³⁻ content as % of P _T ^a (±0.8)	Atomic ratio Ca/P _T (±0.01)
10	9.4	1.50
100	9.3	1.49
5000	6.3	1.53

Liquid/solid weight ratio	HPO ₄ ³⁻ content as % of P _T ^a (±0.8)	Atomic ratio Ca/P _T (±0.01)
10	9.4	1.50
100	9.3	1.49
5000	6.3	1.53

^a P_T is the total phosphorus.

The data obtained clearly indicate that the apatitic phase which is formed at the end of treatment does not depend on the pre-heating of the ATCP. For every sample, the poorly crystalline apatite phases formed show close characteristics.

4.2. Enthalpy variations during the hydrolytic treatment

Contrary to the results of the chemical analysis, the heat flow during hydrolytic treatment and the kinetic of the apatitic-conversion depends strongly on the pre-heating of the initial amorphous phase (Table 2). On the microcalorimetric curves (Fig. 1) two main exothermic peaks, and sometimes a weak non-quantifiable endothermic phenomenon were observed.

4.2.1. The first peak

The first exothermic peak which begins instantaneously on immersion of the powder in water can be assigned to a wetting phenomenon corresponding to the fast hydration of the surface of the ATCP powder particles.

Moreover, the results of the chemical analyses of the hydrolysis solutions highlighted that an apparent equilibrium of ATCP dissolution has been reached during an interval not exceeding 30 min after the beginning of the immersion (Fig. 7). This duration is completely included in that of the first peak recorded by microcalorimetry (Table 2). Consequently, the latter corresponds to the superposition of two phenomena: dissolution and wetting.

According to Christoffersen [31] the enthalpy released during the dissolution of one calcium mole of the lyophilized ATCP is -21 kJ at 30–42 °C and it becomes more exothermic when the experimental temperature decreases. Considering the quantity of calcium in the solution, the

enthalpy variation due to dissolution of the ATCP_{ly} should be less than 0.04 J, for the mass of ATCP_{ly} used in the experiment (40 mg), which represents about 8% of the first peak. For pre-heated ATCPs, dissolution is weaker than that of the lyophilized product [32]. It can be concluded that the first peak essentially represents the wetting enthalpy. It can be noticed that the wetting enthalpy is practically the same for all samples in accordance with their very similar specific surface areas determined by nitrogen adsorption BET [32]: 81, 80 and, 83 (± 4) $\text{m}^2 \text{g}^{-1}$ for ATCP_{ly} , ATCP_{200} and ATCP_{400} , respectively.

4.2.2. The second peak and the endothermic peak

The second peak is three to sixteen times more intense than the first (Table 2). This peak obviously corresponds to the exothermic conversion of the amorphous phases into crystalline apatite. However, the heat release strongly depends on the preliminary thermal treatment of the ATCP phases. This result cannot be due to the formation of intermediate metastable phases or to differences in the final hydrolysis products as the chemical characteristics of the final apatitic phases are all quite similar. Consequently, the dissimilarities recorded by microcalorimetric data seem to be mainly related to the initial ATCP phases.

In recent work concerning the study of the structural evolutions of ATCPs during pre-heating [32], we have shown that pre-heating of ATCP did not seem to involve any structural modification of the amorphous phase but altered its water content. The main difference between the lyophilized and pre-heated ATCP samples is their water content and indeed, when the quantity of water decreases, a considerable decrease of the second peak enthalpy is noticed. This observation suggests that the crystalline transformation (crystallization and hydrolysis of 10% total PO_4^{3-} into HPO_4^{2-}) is superimposed on an exothermic rehydration of the pre-heated amorphous solids particles. The TGA results confirmed the existence of a rehydration process for the pre-heated samples. Assuming that the crystalline transformation of the lyophilized sample represents only the conversion of hydrated ATCP into hydrated apatite, the excess of standard enthalpy released by the rehydration of the pre-heated samples can be calculated. It reaches -36.4 (± 1.3) and -38.6 (± 1.3) kJ mol^{-1} for ATCP_{200} and ATCP_{400} , respectively. These values are higher than that due to crystalline transformation only (-28.4 ± 0.7 kJ mol^{-1} for ATCP) but the difference between the two pre-heated samples seems relatively low. Thus, the large difference in the rates of transformation between the two pre-heated samples can be assigned to the kinetic parameters related to the water diffusion into ATCP particles.

The amount of water re-entering the pre-heated ATCPs can be evaluated using the average hydration standard enthalpy at 25 °C determined in a previous study on the same kind samples: -12.3 (± 1.5) kJ mol^{-1} of liquid water [32]. The amount of water re-entering inner ATCPs particles, calculated from the second peak enthalpy excess is close to 15.4 (± 2.2) and 16.5 (± 2.4) wt% for ATCP_{200} and ATCP_{400} , respectively. If the residual water of the initial ATCPs found with TGA and the wetting water calculated from the first peak are added to the above values, the total maximum hydrating rate necessary for the hydrolytic conversion of each ATCP into apatite will be determined. This calculated amount is close to 21.7 (± 3.2), 23.9 (± 3.5) and 22.1 (± 3.2) wt% for ATCP_{ly} , ATCP_{200} and ATCP_{400} , respectively. It can be noticed that the hydration ratio reached by the pre-heated ATCPs are similar to that of the lyophilized ATCP considering the experimental error.

In addition, the values of the total water uptake calculated from the calorimetric data are higher than the maximal water content determined by TGA in the lyophilized solids obtained during the hydrolytic treatment (Fig. 6) and also higher than the residual water in the original lyophilized ATCP sample. In fact the TGA data give the water content of the samples after partial or total

conversion and lyophilization and do not represent the cumulated water of the re-hydrated ATCP in aqueous media during the apatitic conversion, which is deduced from microcalorimetric data.

Moreover, at the end of the conversion, a decrease of the amount of water associated with the samples as been observed by TGA. This phenomenon seems to correspond to a loss of water from the crystalline apatitic samples.

It has been shown [51] that nascent apatite crystals exhibit, on their surface, a structured hydrated layer corresponding to non-apatitic environments. During aging in solution, this layer progressively becomes diminished and transformed into apatite. The IR data confirm the decrease of the non-apatitic environments after conversion. It can be suggested that this weak endothermic peak sometimes observed at the end of the conversion can be related to the dehydration observed by TGA; that would be a necessary step for growth of crystallites in the maturation process. The observation of this event seems blurred as the conversion lasts longer and the apatite crystals formed have already partly matured before the end of the total transformation of ATCP into apatite. Thus, the endothermic peak decreases and eventually disappears, hindered by the extended exothermic events in pre-heated ATCP.

The enthalpy values which were obtained for the conversion of the lyophilized sample are much larger than those reported by Heughebaert and Guegan [29], [30] and [39] for the conversion of a gel-like sample, which has globally been found to be endothermic whereas we always observed a strong exothermic effect as expected for this natural evolving closed-system. This difference could be assigned partly to a slow rehydration of the lyophilized sample and also possibly to a lower endothermic internal-hydrolysis enthalpy, considering the low amount of HPO_4^{2-} ions in our samples, but at this stage it seems difficult to comment more on this difference.

The hydrolytic conversion of ATCP evidences two exothermic events related to hydration. The first is a fast but rather weak wetting process, and the second, much slower and more intense, lasts considerably longer as the heating temperature of the ATCP is higher. The first phenomenon simply corresponds to the wetting of the external surface of the ATCP particles. The second phenomenon could involve the structure of ATCP itself.

ATCP has been described as an association of water and $\text{Ca}_9(\text{PO}_4)_6$ clusters (often called Posner's clusters) which have been shown to exhibit a particular stability [58] and [59] and are found in most calcium phosphate crystalline phases. These clusters are associated to form larger particles exhibiting a much lower surface area than that which can be calculated from isolated clusters [32]. The fast wetting reaction can be associated with the rehydration of the particles whereas the slower rehydration process could be related to the slow diffusion of water in the particles and the hydration of the clusters. The amount of water associated with hydrated ATCP can be evaluated to about 12 water molecules per $\text{Ca}_9(\text{PO}_4)_6$ unit (based on the assumptions made above).

The mechanism of hydrolysis is however obscure. For some authors, the conversion of ATCP into apatite is related to a dissolution–reprecipitation phenomenon and depends on conditions existing in the solution [4], [5] and [52], for others [29], [30] and [39] it appears as an internal restructuration phenomenon where the hydrolysis of PO_4^{3-} units and the formation of OH^- ions is the crucial event leading to a rearrangement of the ATCP particles. It should be noticed however that these authors were studying different systems with very different liquid-to-solid ratios and different pHs. The data presented here do not bring a clear answer. The Posner's clusters, have been shown to exhibit a peculiar stability [59] and [60] and the complete destruction of these units in ATCP to rebuild the HA structure would probably correspond to a high activation energy. Thus a reorganisation of these units to build the apatite structure seems probable. However, the solution is supersaturated with respect to the different Ca–P phases and a dissolution–reprecipitation necessarily occurs when both phases are in contact with an aqueous medium. In fact both mechanisms may exist depending on the respective rates of dissolution and reprecipitation

compared to hydrolysis and restructuring.

ATCP is involved in several biomaterials, especially HA plasma-sprayed coatings. This coating process induces a fusion and a partial decomposition of the HA and the resulting coating may contain up to 50% amorphous phase. Although the composition of this phase is not the same as ATCP [61], it can be reasonably considered that its hydration implies a strong release of heat, and a probable volume increase due to water incorporation. These phenomena could be responsible—at least partly—for the formation of cracks when the coatings are immersed in water [62], although the reaction of water with calcium oxide residue could also be involved. Despite its negative effect on the coating integrity, the hydrolysis of the amorphous phase has been suggested to be related to biological properties [11], [12], [13], [14], [15] and [16]. Data obtained in simulated body fluid (SBF) indicate the formation of a bone-like apatitic layer on the coating considered to be related to its biological performance [63]. The formation of this layer has often been interpreted as dissolution of the amorphous phase and a precipitation of apatite from the supersaturated solution. The ionic-products of ATCP solutions obtained in this work indicate that SBF is effectively undersaturated with respect to the amorphous phase and justifies its dissolution. However, a slow rehydration process of the amorphous phase in the coatings and its reorganization into apatite nanocrystals cannot be excluded. One crucial question is the rehydration ability of the ATCP phase. ATCP binds water molecules strongly and they are only slowly released by heating at high temperature (up to 500 °C). Rehydration of ATCP from aqueous solutions or even atmospheric humidity could slowly modify the coatings characteristics and their biological behavior.

5. Conclusion

The hydrolysis of dry ACP is dominated by two strong exothermic events a fast hydration reaction related to the immersion of the mineral surface in water and a slow but stronger heat release due to a slow hydration reaction corresponding to the penetration of water molecules into the amorphous particles. The conversion time of the amorphous phase into apatite increases considerably as the degree of hydration of the amorphous phase decreases. The nascent nanocrystalline apatitic phase evolves with time after its formation. The crystallinity and the OH⁻ content increase whereas the amount of HPO₄²⁻ ion decreases. Two processes are probably involved in the conversion of the amorphous phase into apatite: dissolution–reprecipitation and restructuring of the stable Posner's clusters. The relative importance of these mechanisms could explain the discrepancies between data of different authors. Dissolution–reprecipitation could be favored at high liquid-to-solid ratios and restructuring at low liquid-to-solid ratios, like in Ca–P cements involving ATCP.

Acknowledgment

The authors thank J. Lacaze from ENSIACET (France) for his help in the DTA.

References

- J.D. Termine and A.S. Posner, *Science* **153** (1966), pp. 1523–1525.
M.D. Grynpas, L.C. Bnar and M.J. Glimcher, *J. Mater. Sci.* **19** (1984), pp. 723–736.

- K. Simkiss, *Bull. l'Inst. Océanograph. No spécial* **14** (1994), pp. 49–54.
- J.A. Szivek, P.L. Anderson, T.J. Dishongh and D.W. DeYoung, *J. Biomed. Mater. Res.* **33** (1996), pp. 121–132.
- M. Nagano, T. Nakamura, T. Kokubo, M. Tanahashi and M. Ogawa, *Biomaterials* **17** (1996), pp. 1771–1777.
- R. Yates, J. Owens, R. Jackson, R.G. Newcombe and M.J. Addy, *Clin. Periodontol.* **25** (1998), pp. 687–692.
- M.S. Tung, F.C. Eichmiller, *J. Clin. Dent.* **10**(1), special number- (1999) 1–6.
- J.M. Winterbottom, L. Shimp, T.M. Boyce, D. Kaes, Implant, method of making same and use of the implant for the treatment of bone defects, US Patent No. 6,478,825, 2002.
- D. Lee, C. Rey, M. Aiolova, A. Tofighi, Methods and products related to the physical conversion of reactive amorphous calcium phosphate, US Patent No. 08/729,344, 1996.
- D. Skertic, J.M. Anttonucc, E.D. Eanes, F.C. Eichmiller and G.E. Schumacher, *J. Biomed. Mater. Res. Appl. Biomater.* **53** (2000), pp. 381–391.
- H.A. Lowenstam and S. Weiner, *On Biomineralization*, Oxford University Press, New York (1989).
- S.H. Maxian, J.P. Zawadsky and M.G. Dunn, *J. Biomed. Mater. Res.* **27** (1993), pp. 717–728.
- C.A. Van Blitterswijk, Y.P. Bowell, J.S. Flach, H. Leenders, I. van den Brink and J. de Bruijn In: R.G.T. Geesink and M.T. Manley, Editors, *Hydroxapatite Coatings in Orthopodic Surgency*, New York (1993), pp. 33–47.
- J.D. de Bruijn, Y.P. Bovell and C.A. van Blitterswijk, *Biomaterials* **15** (1994), pp. 543–550.
- J.A.M. Clemens, J.G.C. Wolke, C.P.A.T. Klein and K. de Groot, *J. Biomed. Mater. Res.* **48** (1999), pp. 741–748.
- X. Weichang, T. Shunyan, L. Xuanyong, Z. XueBin and D. Chuanxian, *Biomaterials* **23** (2004), pp. 415–421.
- F. Garcia, J.L. Arias, B. Mayor, J. Pou, I. Rehman, J. Knowles, S. Best, B. Leon, M. Perez-Amor and W. Bonfield, *J. Biomed. Mater. Res.* **43** (1998), pp. 69–76.
- D. Shinn-jyh, H. Tsui-hsien and K. Chia-tze, *Surf. Coat. Technol.* **16** (2003), pp. 248–257.
- D. Knaack, M.E.P. Goad, M. Ailova, C. Rey, A. Tofighi, P. Chakravarthy and D. Lee, *J. Biomed. Mater. Res.* **43** (1998), pp. 399–409.
- A. Tofighi, S. Mounic, P. Chakravarthy, C. Rey and D. Lee, *Eng. Mater.* **192–195** (2001), pp. 769–772.
- E.D. Eanes, J.H. Gillessen and A.S. Posner, *Nature* **208** (1965), pp. 365–367.
- N.C. Blumenthal and A.S. Posner, *Calcif. Tissue Res.* **13** (1973), pp. 235–243.
- J.L. Meyer, *Croatica Chim. Acta* **56** (1983), pp. 753–767.
- M.S. Tung and W.E. Brown, *Calcif. Tissue Int.* **35** (1983), pp. 783–790.
- J. Christoffersen, M.R. Christoffersen, W. Kibalczyk and F.A. Andersen, *J. Crystal Growth* **94** (1989), pp. 767–777.
- In: J.C. Elliott, Editor, *Structure and Chemistry of the Apatite and Other Calcium Orthophosphates Studies in Inorganic Chemistry 18*, Amsterdam, London, NewYork, Tokyo, Elsevier (1994).
- S. Habelitz, L. Pascual and A. Duran, *J. Mater. Sci.* **36** (2001), pp. 4131–4135.

- E.D. Eanes, *Calcif. Tissue Res.* **5** (1970), pp. 133–145.
- C. Guegan, contribution à l'étude cinétique de l'évolution de l'état apatitique des orthophosphates tricalciques (Ca,Mg) précipités, Thesis INP Toulouse, 1978.
- J.C. Heughebaert and G. Montel, *Calcif. Tissue Int.* **34** (1982), pp. S103–S108.
- M.R. Christoffersen and J. Kibalczyk, *J. Crystal Growth* **106** (1990), pp. 349–354.
- S. Somrani, C. Rey and M. Jemal, *J. Mater. Chem.* **13** (2003), pp. 888–892.
- E.D. Eanes and A.S. Posner, *Trans. NY Acad. Sci.* **28** (1965), pp. 233–241.
- A.G. Walton, W.J. Bodin, H. Furedi and A. Schwartz, *Can. J. Chem.* **45** (1967), pp. 2695–2701.
- P. Layrolle, Synthèse de phosphates de calcium en milieu organique, Thesis INP Toulouse, 1994.
- R.E. Wuthier, G.S. Rice, J.E.B. Wallace Jr., R.L. Weaver, R.Z. Legeros and E.D. Eanes, *Calcif. Tiss. Int.* **37** (1985), pp. 401–410.
- A. Lebugle, E. Zahidi and G. Bonel, *Reactivity of Solids* **2** (1986), pp. 151–161.
- Layrolle and A. Lebugle, *Chem. Mater.* **6** (1994), pp. 1996–2004.
- J.C. Heughebaert, Contribution à l'étude de l'évolution des orthophosphates de calcium précipités amorphes en orthophosphates apatitiques, Thesis INP Toulouse, 1977.
- E. Calvet, H. Prat, Masson, Cie (Eds.), *Microcalorimétrie, Application Physico-Chimique et Biologique*, Paris, 1956.
- P. Scherrer, *Gött Narch* **2** (1918), p. 98.
- C.F. Feng, K.A. Khor, S.W.K. Kweh and P. Cheang, *Mater. Lett.* **46** (2000), pp. 229–233.
- In: G. Charlot, Editor, *Les méthodes de la chimie analytique Analyse Qualitative et minérale*, Mason, Paris (1966).
- A. Gee and V.R. Deitz, *J. Am. Chem. Soc.* **77** (1955), pp. 2961–2965.
- E.W.D. Huffman, *Microchem. J.* **22** (1977), pp. 667–673.
- J. Christofferson, M.A. Christofferson, W. Kibalczyk and F.A. Anderson, *J. Crystal Growth* **94** (1989), p. 767.
- J.D. Termine and E.D. Eanes, *Calcif. Tissue Res.* **10** (1972), pp. 171–197.
- J.L. Meyer and E.D. Eanes, *Calcif. Tissue Res. A* **25** (1978), pp. 59–68.
- C. Combes, C. Rey and S. Mounic, *Eng. Mater.* **192–195** (2001), pp. 143–146.
- J.D. Termine, R.A. Peckauskas and A.S. Posner, *Arch. Biochem. Biophys.* **140** (1970), pp. 318–325.
- L.C. Bonar, A.H. Roufousse, W.K. Sabine, M.D. Grinpas and M.J. Glimcher, *Calcif. Tissue Int.* **35** (1983), pp. 202–209.
- A.L. Boskey and A.S. Posner, *J. Chem. Phys.* **80** (1976), pp. 40–45.
- L.C. Chow, in: L.C. Chow, E.D. Eanes (Eds.), *Octacalcium Phosphate: Monographs in Oral Science*, G.M. Whitford (Ed.), KARGER, Basel, 2001, Vol. 18, pp. 94–111.
- P.G. Koutsoukos and G.H. Nancollas, *J. Crystal Growth* **53** (1981), pp. 10–19.
- G.R. Sauer and R.E. Wuthier, *J. Biol. Chem.* **263** (1988), pp. 13,718–13,724.
- S. Gregory Makowski and L. Melinda Ramsby, *Inflammation* **23** (1999), pp. 333–360.
- J.L. Meyer and C.C. Weatherrall, *J. Colloïd Interf. Sci.* **89** (1982), pp. 257–267.

F. Betts and A.S. Posner, *Trans. Crystal Assoc.* **10** (1974), pp. 73–80.

G. Treboux, P. Layrolle, N. Kanzaki, K. Onuma and A. Ito, *J. Phys. Chem.* **104** (2000), pp. 5111–5114.

N. Kanazaki, G. Treboux, K. Onuma, S. Tsutsumi and A. Ito, *Biomaterials* **22** (2001), pp. 2921–2929.

M.T. Carayon and J.L. Lacout, *J. Solid State Chem.* **172** (2003), pp. 339–350.

J. Weng, J.G.C. Wolke, X. Zhang and K. de Groot In: J. Wilson, L. Hench and D. Greenspan, Editors, *Bioceramics 8*, Pergamon, Elsevier, Oxford (1994), pp. 339–344.

J. Weng, Q. Liu, J.G.C. Wolke, X. Zhang and K. de Groot, *Biomaterials* **18** (1997), pp. 1027–1035.

Corresponding author. Fax: +33 05 62 88 57 73.

Original text : Elsevier.com